Modeling *a priori* Unknown Environments: Place Recognition with Optical Flow Fingerprints

Zachary Mueller and Sotirios Diamantas
Department of Engineering and Computer Science, Tarleton State University, Texas A&M University System, Box T-0390, Stephenville, TX 76402, U.S.A.

Keywords: Place Recognition, Optical Flow, Optical Flow Fingerprints, Loop Closing.

Abstract: In this research we present a novel method for place recognition that relies on optical flow fingerprints of features. We make no assumptions about the properties of features or the environment such as color, shape, and size, as we approach the problem parsimoniously with a single camera mounted on a robot. In the training phase of our algorithm an accurate camera model is utilized to model and simulate the optical flow vector magnitudes with respect to velocity and distance to features. A lognormal distribution function, that is the result of this observation, is used as an input during the testing phase that is taking place with real sensors and features extracted using Lucas-Kanade optical flow algorithm. With this approach we have managed to bridge the gap between simulation and real-world environments by transferring the output of simulated training data sets to real testing environments. In addition, our method is highly adaptable to different types of sensors and environments. Our algorithm is evaluated both in indoor and outdoor environments where a robot revisits places from different poses and velocities demonstrating that modeling an unknown environment using optical flow properties is feasible yet efficient.

1 INTRODUCTION

This research shows how to develop a model that estimates the probability of having revisited the same place or site based on optical flow patterns. In order to accomplish this we do this in two phases, training and testing. The training phase is solely carried out on a simulator, drastically reducing both time and work in the estimation process. In addition, our method is adaptable to different types of environments as well as camera sensors. This research shows that it is possible to train a model in a simulator and to then use the simulated output as input during the testing phase for real-world environments. The simulated results rely on accurate camera calibration and motion and distance parameters between camera and features. The training phase which is based on simulation acts complementary to the training phase which is taking place with real-world camera and robotic systems. A similar training data set has also been used in (Diamantas et al., 2010) where results obtained using a simulation engine only.

In the training sessions we consider only two parameters, the velocity of the robot and the distance between the robot and the target landmark. By generating optical flow patterns each time the robot is entering and leaving an area, we is able to compare and recognize areas that we have been in before, even when entering the area from different angles or velocities. Then, based on the training done via simulator, a similarity score is produced. This method of re-visiting a site is similar to the method that insects utilize in nature when entering or exiting an area.

Place recognition has always been a fundamental problem in robotics and computer vision. A robot that is capable of recognizing a previously unknown environment is in great need, as this capability is interwoven with localization and mapping problems in robotics science. Place recognition using visual information has attracted much attention the last few years especially since the advent of algorithms that are robust to scaling and camera orientation (Lowe, 1999), (Bay et al., 2008b). While optical flow has become a popular topic in the last decades, there has been no research done previously for place recognition using optical flow *fingerprints*. Most place recognition research is done using properties of the environment, while optical flow uses the property of the camera motion, and is a function of the velocity of the camera and the distance between the camera and the object.

Mueller, Z. and Diamantas, S.
Modeling a priori Unknown Environments: Place Recognition with Optical Flow Fingerprints.
DOI: 10.5220/0010271007930800
In *Proceedings of the 16th International Joint Conference on Computer Vision, Imaging and Computer Graphics Theory and Applications (VISIGRAPP 2021) - Volume 5: VISAPP*, pages 793-800
ISBN: 978-989-758-488-6

Optical flow is the rate of change of image motion, which is obtained from the motion of the autonomous agent. In both the simulator and on the robot, the camera is placed perpendicular to the direction of motion, so a translational optic flow is generated. Since the optic flow only uses two parameters, all other information is not considered. This allows for the environment that the robot is in to be unknown and unstructured.

Previous works used a simulation to model the deviation of an optical flow vector, using distance and velocity (Diamantas et al., 2010; Diamantas et al., 2011). Building upon that, our current model trains using vector magnitudes that vary with respect to distance and velocity. When testing in the real-world environment we are using a *Dr Robot 4x4* mobile robot equipped with a *Blackfly S USB3* camera.

Optical flow is a method that is inspired by biology, specifically by the way honeybees use optical flow for navigation and obstacle avoidance. Biological inspiration provides solutions to common problems that robots encounter. By utilizing optical flow we gain multiple advantages. First, we gain algorithmic simplicity and performance, which in turn saves on power consumption. Second, we gain insight into the biological organisms that will, in turn, help us perceive and understand the underlying mechanisms that facilitate biological organisms (Diamantas, 2010). The final advantage to using optical flow is that we do not store the images used, only the optical flow patterns. This removes image retrieval times, and processing between images is not required. This further contributes to the time efficiency of this method.

This paper comprises four sections. Following is Section 2 where work on optical flow is presented. In Section 3 the methodology of the probabilistic model that is divided into the training phase and the testing phase is presented. Results are also presented in this section from experiments carried out both in indoor and outdoor environments with the robot re-visiting places at varying velocities and distances. Finally, Section 4 epitomizes the conclusions drawn from this research and indicates a number of areas that further research is attainable.

2 RELATED WORKS

Optical flow has been a topic for research for several decades. One of the first works that studied the relation of scene geometry and the motion of the observer was by (Gibson, 1974). A large amount of work, however, has been focused on obstacle avoidance using optical flow (Camus et al., 1996; Warren and Fajen, 2004; Merrell et al., 2004). The technique, generally, works by splitting the image (for single camera systems) into left and right sides. If the summation of vectors of either side exceeds a given threshold then the vehicle is about to collide with an object. Similarly, this method has been used for centering autonomous robots in corridors or even a canyon (Hrabar et al., 2005) with the difference that the summation of vectors must be equal in both the left-hand side and the right-hand side of the image. (Ohnishi and Imiya, 2007) utilize optical flow for both obstacle avoidance and corridor navigation. (Madjidi and Negahdaripour, 2006) have tested the performance of optical flow in underwater color images.

In a work implemented by (Kendoul et al., 2009) optic flow is used for fully autonomous flight control of an aerial vehicle. The distance travelled by UAV is calculated by integrating the optic flow over time. A similar work for controlling a small UAV in confined and cluttered environments has been implemented by (Zufferey et al., 2008). (Barron et al., 1994) discuss the performance of optical flow techniques and their comparison and focused on accuracy, reliability and density of the velocity measurements.

Visual recognition and comparisons through imaging can be broken down into roughly three categories, while many algorithms utilize these categories in tandem.

2.1 SURF/SIFT Tracking

Relying on local features, SURF (Speeded-Up Robust Features)(Bay et al., 2008a) allows for finding point similarities between two separate images. After identifying 'interest points' that are repeatedly findable, the detector can then be used in multiple images and matched between them. The matching is done based on distance vectors. The matching time of distance vectors has to find a balance between the dimensions of the descriptor. A descriptor with few dimensions is better for fast identification and matching, but a descriptor with fewer dimensions is also less distinctive and can result in false positives. SIFT tracking (Scale Invariant Feature Transform) (Lowe, 1999) uses similar local feature vectors, and is invariant to lighting changes and image translation, scaling, and rotation. By using staged filtering, the SIFT tracking identifies its interest points by finding local maxima and minima, and each point is used to generate a feature vector, which is easily searchable and comparable. In (Bardas et al., 2017) a monocular camera is employed to track and classify objects.

2.2 Scene Text Tracking

Scene text tracking (Liao et al., 2018) relies primarily on written word throughout images, in order to determine geolocation. The process of identifying text (Wang et al., 2015) is challenging because of the vast variations in how the text is presented. Combine that with varied lighting, orientations, and angles, the process of identifying text is a difficult one, but not one that can't be overcome. Once text is identified, it can then be used to compare between multiple images. While this technology is available publicly (Liao et al., 2017), it has shortcomings when used in environments that do not have text widely displayed.

2.3 Deep Learning

While some algorithms do not require similar lighting situations, others still require similar scenarios for the images to be compared accurately. Night-to-Day Image translation (Jégou et al., 2010) allows for images taken at night to be cast into possible images from a daytime perspective. This can then be used to compare images in a database of geo-tagged images to find the prospective location of the image. The process of Night-to-Day translation uses a neural model that takes relatively little training and does not require ground-truth pairings. Alongside image translation, there is the prospect of comparing images against all other images in a database. BOF (Bag-Of-Features)(Draper, 2011) search is a new approach to optimize searching, with results that optimize the image representation and allow for quick results on large datasets. Similarly, using a FAB-MAP (Cummins and Newman, 2008) tackles the problem of recognizing places based off of appearance, despite subtle differences between images. To accomplish this there are learned generative models, and new models can be learned online using a single observation. The benefit to FAB-MAP is the linear complexity in the number of places in the map.

3 METHODOLOGY

This section describes the methodology followed for tackling the place recognition problem using optical flow *fingerprints*. Our approach is divided into training and testing phases. Initially, we calibrate our camera, a *FLIR Blackfly S*, to estimate the intrinsics parameters of the camera (Fig. 1). The intrinsics parameters are utilized to build an accurate model of the camera and simulate 3D points at varying distances from the camera taken with inconstant mobile robot velocities. These 3D points, using the camera model, are projected onto the 2D plane. During the training phase we observe the variability of the optical flow vector magnitudes and how these change with respect to distance and velocity. The training phase which is simulation-based is carried out offline. In addition, using an accurate model of the camera we can simulate a very large number of 3D points that would otherwise be impossible to observe using real-world points and data. This entails a very descriptive probability distribution function that describes the relationship between distance and velocity.

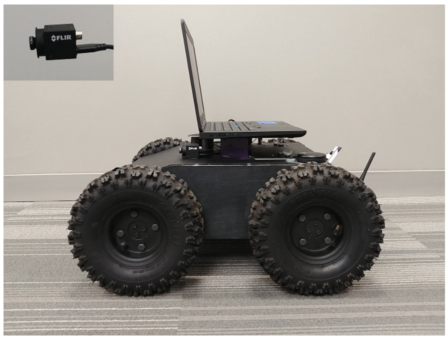

Figure 1: Dr. Robot Jaguar mobile robot platform with FLIR Blackfly S camera onboard.

In our approach we employ the Lucas-Kanade optical flow algorithm (Lucas and Kanade, 1981) which is a sparse optical flow technique entailing in a faster computation of motion vectors. In this research we have used a single camera to implement optical flow and recognize places from the optical flow patterns. The camera is mounted on a mobile robot platform (Fig. 1) along with a laptop computer with quad-core *Intel Core i7-8650U* processor and 16GB of RAM. No other sensors are utilized in this research. In addition, apart from the intrinsics of the camera no other parameters are known. Camera velocity and distance to 3D points are modeled during the training phase, however, these two parameters are unknown during testing phase.

3.1 Training Phase

During the training phase we observe the magnitude variability of optical flow vectors with respect to velocity and distance. The mean and standard deviations for velocity and distance are summarized in Table 1. Both velocity and distance are drawn from Gaussian probability distribution functions. The parameters for velocity and distance used reflect the corresponding parameters for velocity and depth in indoor and outdoor environments where the mobile robot navigates with a relatively low velocity and the distance to features is small in an indoor environment while the velocity and distance are higher when navigating through an outdoor environment .

Table 1: Modeling Parameters for Indoor and Outdoor Environments.

	Indoor	Outdoor
Distance (m)	$\mu = 1.5$ $\sigma = 0.4$	$\mu = 20.0$ $\sigma = 5.0$
Velocity (km/m)	$\mu = 1.3$ $\sigma = 0.3$	$\mu = 3.45$ $\sigma = 1.0$

Figure 2 provides a pictorial representation of the Gaussian distributions used for modeling camera velocities and distances between camera and 3D points (Fig. 3). We have observed 1 million, $n = 10^6$, 3D features with varying depths and velocities at which they are observed. The overall simulation and projection of 3D points onto the 2D image plane of the modeled camera required about 14.5 minutes (on a quad-core *Intel Core i7-8650U* processor with 16GB of RAM). For modeling the *FLIR Blackfly S* camera we employed the (Corke, 2011) toolbox. Equation 1 shows the mathematical formulation for computing the mean magnitude, $||\vec{u}||$, of all vectors given the $n = 10^6$ 3D points

$$\vec{v} = \frac{1}{n} \cdot \sum_{k=1}^{n} ||\vec{u}_k|| \quad n = 1000000. \tag{1}$$

The mean length, $\vec{v}$, of the n optical flow vectors is then subtracted from each one of the n optical flow vectors as shown in (2)

$$X_k = |\vec{v} - ||\vec{u}_k||| \tag{2}$$

The resultant histogram derived by (2) is described by a lognormal probability density function (pdf) as expressed by (3)

$$f_X = (\delta; \mu, \sigma) = \frac{1}{\delta\sigma\sqrt{2\pi}} e^{-\frac{(\ln\delta-\mu)^2}{2\sigma^2}} \quad \delta > 0. \tag{3}$$

The lognormal pdf acts as a likelihood estimator for correlating the optical flow patterns between the training and testing phases. For inferring the probabilistic score between the two patterns the cumulative density function of the lognormal function is used and, as expressed in (4)

$$F_X(\delta; \mu, \sigma) = \frac{1}{2} erfc\left[-\frac{\ln\delta - \mu}{\sigma\sqrt{2}}\right] = \Phi\left(\frac{\ln\delta - \mu}{\sigma}\right). \tag{4}$$

Further to this, following our methodology any camera can be modeled and the optical flow vectors can be obtained by setting the parameters for velocity and distance. This approach greatly simplifies the modeling of an *a priori* unknown environment. Yet, the parameters for velocity and distance can easily be modified to model and simulate different types of environments on which the robot will navigate, for instance, high-speed traversing of an outdoor environment. The modeled camera and its intrinsic matrix K along with its corresponding values are shown in (5)

$$\begin{bmatrix} f/\rho_w & 0 & u_0 \\ 0 & f/\rho_h & v_0 \\ 0 & 0 & 1 \end{bmatrix} = \begin{bmatrix} 1682.4 & 0 & 757 \\ 0 & 1682.4 & 598 \\ 0 & 0 & 1 \end{bmatrix} \tag{5}$$

The resolution of the specific camera was set to 1440×1080 and the frame rate was approximately 12.3 frames/second. The focal length in mm was estimated to be 5.80 mm, while the pixel size was 3.45×10^{-6} μm and the diagonal field of view (FOV) $\simeq 58.42°$.

Figures 4 (a-b) depict the probability density function (PDF) and the cumulative density function (CDF) of the lognormal function respectively, derived from training using the parameters as shown in Table 1 for an indoor environment. The estimated mean and standard deviation of the training PDF are $\mu = 1.93$ and $\sigma = 1.17$, respectively. In Figs. 4 (a) and (c) the histogram of the PDF depicts the variation of the length of the optical flow vectors with respect to distance and velocity in a sample of 10^6 training repetitions. Figures 4 (c-d) depict the lognormal PDF and CDF for an outdoor environment. The estimated mean and standard deviation of the training PDF are $\mu = 1.87$ and $\sigma = 0.42$.

3.2 Testing Phase

During the testing phase the robot navigates in a *a priori* unknown environment. The distance and velocity of the navigating robot have to comply with the modeled parameters of the training phase. Although this is not a strict rule, observations from the testing environment have shown that the closer the real-world parameters are to the modeled environment the better and more accurate the similarity score will be. During testing, the robot takes continuous snapshots of the environment and generates the optical flow patterns using the Lucas-Kanade optical flow algorithm. No images are stored nor is there a need for image retrieval and comparison, only the properties of the optical flow vectors are stored in each pair of frames.

In particular, during testing the robot passes from the same scene twice. At least two passes are necessary for the robot to identify and recognize a scene.

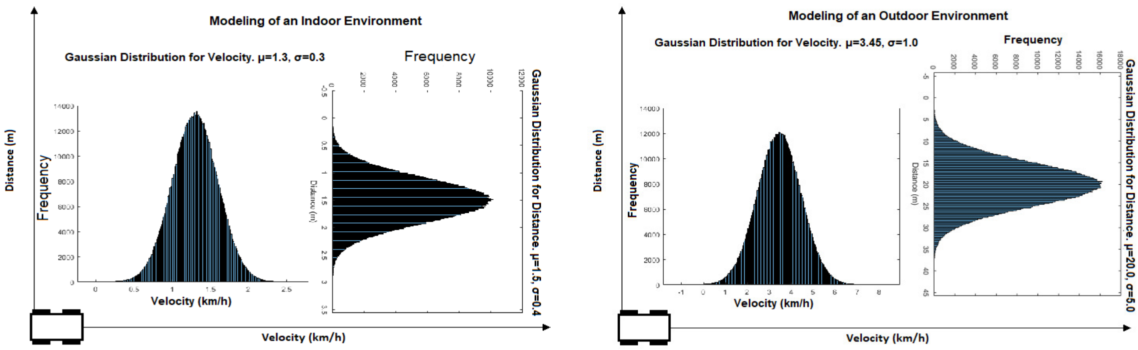

(a) (b)

Figure 2: (a) Gaussian probability distribution functions used for modeling camera velocities and distances to features. The mean and standard deviation for an indoor environment for velocity are $\mu = 1.3$ and $\sigma = 0.3$ whereas mean distance and standard deviation for distance are $\mu = 1.5$ and $\sigma = 0.4$; (b) for an outdoor environment the velocity parameters are $\mu = 3.45$ and $\sigma = 1.0$ whereas for distance are $\mu = 20.0$ and $\sigma = 5.0$.

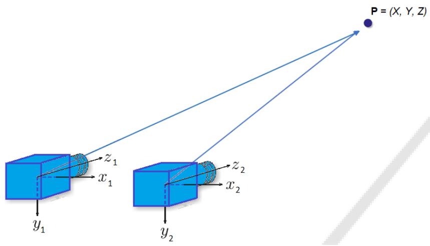

Figure 3: 3D point, **P**, observed by the same camera at two different poses.

In the first pass the robot captures images and generates the optical flow patterns while in the second pass the robot attempts to identify and recognize whether a scene has previously been visited by the robot by comparing the optical flow patterns based on the lognornal distributions generated during the training phase. The problem of place recognition is also referred to as close looping where a robot tries to recognize a scene when the robot closes the loop (second pass). In the first pass we compute the midpoint of each one of the vectors and then we compute the midpoint of all midpoints, as shown in 6

$$\bar{x_i}, \bar{y_i} = \frac{1}{r} \cdot \sum_{a=1}^{r} x_a, y_a \tag{6}$$

In the second pass, we again compute the midpoint of all midpoints as described by 7

$$\bar{x_j}, \bar{y_j} = \frac{1}{s} \cdot \sum_{b=1}^{s} x_b, y_b \tag{7}$$

Finally, we compute the Euclidean distances (eqn. 8) between the two optical flow patterns (through their midpoints) and we plug the result of it, δ, into our Cumulative Distribution Function derived from the training data set which computes the similarity score between the first pass and the second pass.

$$\delta = \sqrt{(\bar{x_i} - \bar{x_j})^2 + (\bar{y_i} - \bar{y_j})^2} \tag{8}$$

The final similarity score is computed using eqn. 9.

$$P = 1 - P_\delta \tag{9}$$

3.3 Experiments

The following figures present the environments experiments were carried out as well as the results accomplished. Figure 5 shows images of the outdoor site used to carry out place recognition by traversing three different routes depicted with red (first pass) and blue (second pass) vectors. (a) Routes 1 and 2 and (b) route 3. Figure 6 shows images taken by the robot from indoor and outdoor environments under varying velocities and distances. In addition, the brightness of images is not constant across all images. In the first column the reference images are shown while in the rest of columns the images with the highest similarity scores are depicted. In our results, there was only one false positive which is shown in the third row of the second column. The highest similarity scores for two similar images is around 1% (1.76% for indoor images) with a decreasing similarity score for images which are less similar. For dissimilar images the similarity score drops significantly. As it can be seen the similarity score is evidently high when the snapshots are from the vicinity of the reference pose in spite of the variation in velocities between the reference image and the current robot snapshots.

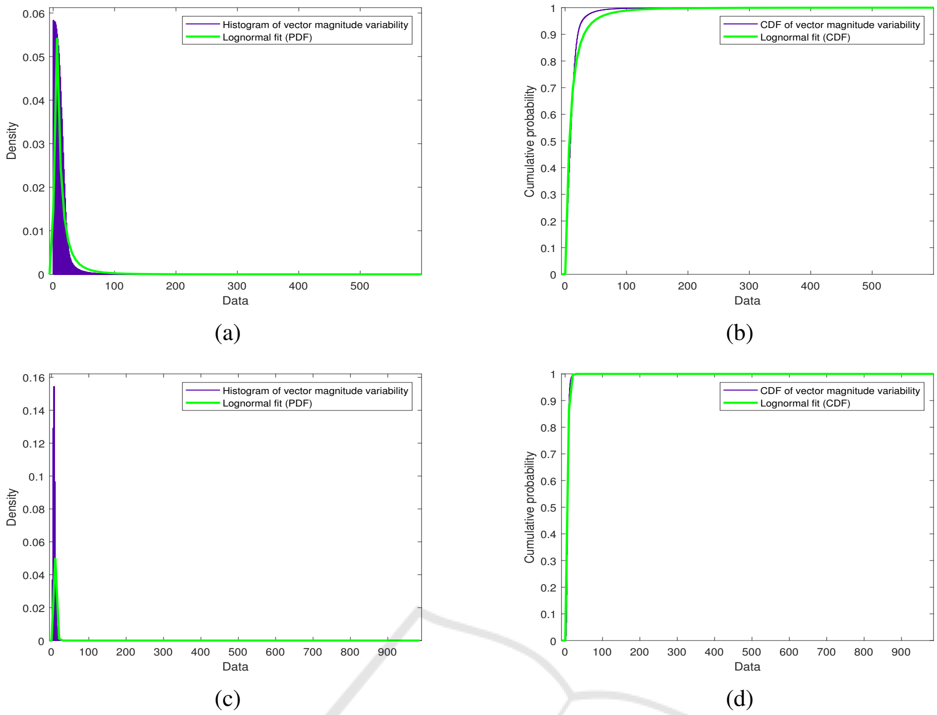

Figure 4: (a-b) Indoor Environment: the histogram expresses the variability of the magnitude of the optical flow vectors with respect to distance and velocity. The fitting functions are expressed with a lognormal Probability Distribution Function (PDF) and a lognormal Cumulative Distribution Function (CDF). Mean and standard deviation are $\mu = 1.93$ and $\sigma = 1.17$, respectively; (c-d) Outdoor Environment: Mean and standard deviation are $\mu = 1.87$ and $\sigma = 0.42$, respectively.

(a) (b)

Figure 5: Outdoor testing environment: Red vectors denote first pass while blue vectors denote a second pass; (a) routes 1 and 2; (b) route 3.

4 CONCLUSIONS AND FUTURE WORK

In this research we have implemented a method for place recognition based on the similarity of optical flow fingerprints. We have shown that using minimal information about the environment as well as the sensors employed it is feasible to model, train, and test a robot to recognize places from the way an environment is perceived and not based on the characteristics or the properties of the environment. In addition, we have managed to exploit the advantages simulation offers such as fast computations using large sample data sets by providing the output of it to real-world experiments.

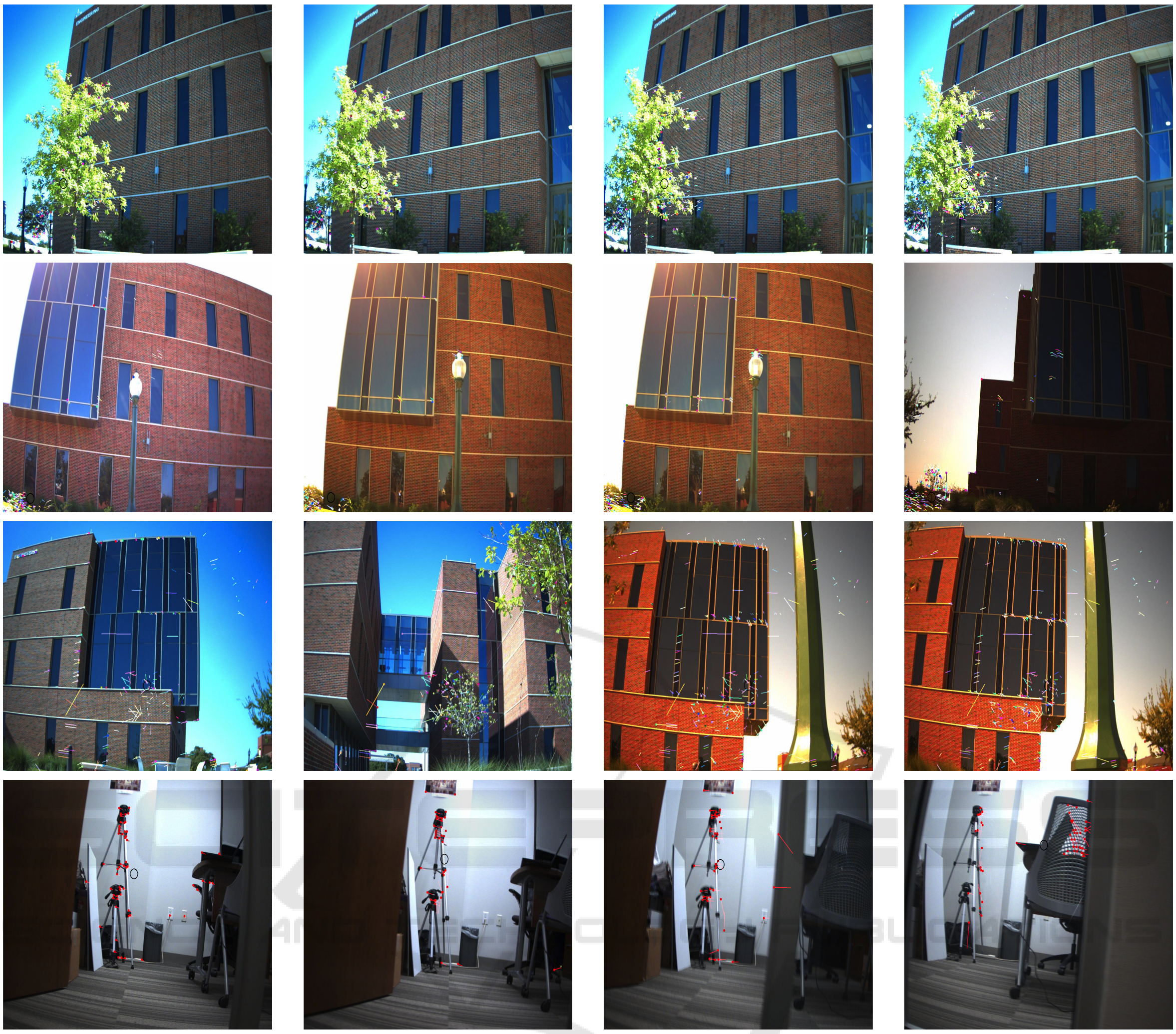

Figure 6: In the first column the reference images are depicted while in columns 2-4 the images with the highest similarity scores are depicted (from high to low). The first three rows are from routes 1-3 while the last row is from an indoor office environment. In the second image of the third row it was the only false positive found. Images were captured with different velocities and distances as well as varying illumination conditions.

As a future work we wish to extend this model in several ways. First, we plan to incorporate into our model methods that will allow the robot to navigate in and recognize dynamic environments. A method we will mostly be considering for dealing with dynamic environments appears in (Cherubini and Chaumette, 2012). Second, we want implement the Kullback-Leibler (KL) divergence for comparing different multivariate probability distribution functions that arise from the optical flow patterns. In that latter case, training may not be necessary.

REFERENCES

Bardas, G., Astaras, S., Diamantas, S., and Pnevmatikakis, A. (2017). 3D tracking and classification system using a monocular camera. *Wireless Personal Communications*, 92(1):63–85.

Barron, J. L., Fleet, D. J., and Beauchemin, S. S. (1994). Performance of optical flow techniques. *International Journal of Computer Vision*, 12(1):43–77.

Bay, H., Ess, A., Tuytelaars, T., and Gool, L. V. (2008a). Speeded-up robust features. *Computer Vision and Image Understanding*, 110(3):346–359.

Bay, H., Ess, A., Tuytelaars, T., and Gool, L. V. (2008b). Surf: Speeded up robust features. *Computer Vision and Image Understanding*, 110(3):346–359.

Camus, T., Coombs, D., Herman, M., and Hong, T.-S.

(1996). Real-time single-workstation obstacle avoidance using only wide-field flow divergence. In *Proceedings of the 13th International Conference on Pattern Recognition*, volume 3.

Cherubini, A. and Chaumette, F. (2012). Visual navigation of a mobile robot with laser-based collision avoidance. *The International Journal of Robotics Research*, 32(2):189–205.

Corke, P. I. (2011). *Robotics, Vision & Control: Fundamental Algorithms in Matlab*. Springer.

Cummins, M. and Newman, P. (2008). Fab-map: Probabilistic localization and mapping in the space of appearance. *The International Journal of Robotics Research*, 27(6):647–665.

Diamantas, S. C. (2010). *Biological and Metric Maps Applied to Robot Homing*. PhD thesis, School of Electronics and Computer Science, University of Southampton.

Diamantas, S. C., Oikonomidis, A., and Crowder, R. M. (2010). Towards optical flow-based robotic homing. In *Proceedings of the International Joint Conference on Neural Networks (IEEE World Congress on Computational Intelligence)*, pages 1–9, Barcelona, Spain.

Diamantas, S. C., Oikonomidis, A., and Crowder, R. M. (2011). Biologically inspired robot navigation by exploiting optical flow patterns. In *Proceedings of the International Conference on Computer Vision Theory and Applications*, pages 645–652, Algarve, Portugal.

Draper, S. O. B. A. (2011). Introduction to the bag of features paradigm for image classification and retrieval. *https://arxiv.org/abs/1101.3354*, pages 1–25.

Gibson, J. J. (1974). *The Perception of the Visual World*. Greenwood Publishing Group, Santa Barbara, CA, USA.

Hrabar, S., Sukhatme, G., Corke, P., Usher, K., and Roberts, J. (2005). Combined optic-flow and stereo-based navigation of urban canyons for a UAV. In *Proceedings of IEEE/RSJ International Conference on Intelligent Robots and Systems*, pages 302–309.

Jégou, H., Douze, M., Schmid, C., and Pérez, P. (2010). Aggregating local descriptors into a compact image representation. In *2010 IEEE Computer Society Conference on Computer Vision and Pattern Recognition*, pages 3304–3311.

Kendoul, F., Fantoni, I., and Nonami, K. (2009). Optic flow-based vision system for autonomous 3d localization and control of small aerial vehicles. *Robotics and Autonomous Systems*, 57(6–7):591–602.

Liao, M., Shi, B., and Bai, X. (2018). Textboxes++: A single-shot oriented scene text detector. *IEEE Transactions on Image Processing*, 27(8):3676–3690.

Liao, M., Shi, B., Bai, X., Wang, X., and Liu, W. (2017). Textboxes: A fast text detector with a single deep neural network. In *AAAI*.

Lowe, D. (1999). Object recognition from local scale-invariant features. In *Proceedings of the International Conference on Computer Vision (ICCV '99)*, pages 1150–1157, Corfu, Greece.

Lucas, B. D. and Kanade, T. (1981). An iterative image registration technique with an application to stereo vision. In *Proceedings of the 7th International Joint Conference on Artificial Intelligence (IJCAI), August 24-28*, pages 674–679.

Madjidi, H. and Negahdaripour, S. (2006). On robustness and localization accuracy of optical flow computation for underwater color images. *Computer Vision and Image Understanding*, 104(1):61–76.

Merrell, P. C., Lee, D.-J., and Beard, R. (2004). Obstacle avoidance for unmanned air vehicles using optical flow probability distributions. *Sensing and Perception*, 5609:13–22.

Ohnishi, N. and Imiya, A. (2007). Corridor navigation and obstacle avoidance using visual potential for mobile robot. In *Proceedings of the Fourth Canadian Conference on Computer and Robot Vision*, pages 131–138.

Wang, H.-C., Finn, C., Paull, L., Kaess, M., Rosenholtz, R., Teller, S., and Leonard, J. (2015). Bridging text spotting and slam with junction features. In *2015 IEEE/RSJ International Conference on Intelligent Robots and Systems (IROS)*, pages 3701–3708.

Warren, W. and Fajen, B. R. (2004). From optic flow to laws of control. In Vaina, L. M., Beardsley, S. A., and Rushton, S. K., editors, *Optic Flow and Beyond*, pages 307–337. Kluwer Academic Publishers.

Zufferey, J.-C., Beyeler, A., and Floreano, D. (2008). Optic flow to control small uavs. In *IEEE/RSJ International Conference on Intelligent Robots and Systems: Workshop on Visual Guidance Systems for small autonomous aerial vehicles*, Nice, France.